Degradation of azo dye C.I. Acid Red 18 using an eco-friendly and continuous electrochemical process

Ali Reza Rahmani[*],[‡], **Kazem Godini**[**],[‡], **Davood Nematollahi**[***], **Ghasem Azarian**[*],[†], **and Sima Maleki**[*]

*Department of Environmental Health Engineering, Faculty of Health and Research Center for Health Sciences,
Hamadan University of Medical Sciences, Hamadan 65319-56784, Iran
**Faculty of Health, Environmental Health Engineering Department,
Ilam University of Medical Sciences, Banganjab Complex, Ilam 67416-5441, Iran
***Faculty of Chemistry, Bu-Ali-Sina University, Hamadan, Zip Code 65174, Iran

Abstract−Continuous anodic oxidation of azo dye C.I. Acid Red 18 by using PbO_2 electrode in aqueous solution was studied. To reach the best conditions of the process, the influence of various operating parameters such as pH, current density, hydraulic retention time (HRT) and dye concentration on the removal rate of chemical oxygen demand (COD) and color, as indexes showing the amount of efficiency, was investigated. The findings showed that, respectively, 99.9% and 80.0% of the dye and COD were removed (at optimized conditions). Mineralization current efficiency results indicated that at the beginning of the reaction mineralization occurred quickly at a low current density, whereas at high amounts the rate of mineralization the efficiency decreased. At the optimum conditions, the majority of COD was removed only with 38.2 kWh/kg COD of energy consumption in 120 min. By controlling $HO^•$/dye concentration ratio via the parameters adjustment, particularly HRT and current density, this system can treat Acid Red 18 well even at high concentrations. Furthermore, the voltammetry study illustrated that electroactive intermediates created during the process were mineralized at current density of 8.6 mA/cm^2.

Keywords: Azo dye Acid Red 18, Anodic Oxidation, Constant Current Electrolysis, Wastewater Treatment

INTRODUCTION

Sewage produced by textile, food, rubber, color solvents, wool, leather, paints plastic, paper, varnishes, medicine, and cosmetic industries, which contains dye compounds, has lately become a major concern because of both mutagenic and carcinogenic impacts [1,2]. Azo dyes constitute 60-70% of synthetic dyes in the mentioned industries [2]. These wastewaters are very stable in the environment and resistant to oxidation and biodegradation. They are also a considerable source of esthetic pollution and disturb the aquatic ecosystem. Photosynthesis and oxygen solubility decrease is resulted from the discharge of wastewaters consisting of dye compounds even at low contents [2-4].

Although azo dye-containing wastewater treatment through physicochemical methods (such as reverse osmosis, membrane filtration, chemical precipitation, coagulation/flocculation, adsorption, membrane systems, even ion exchange process, irradiation and so forth) has benefits, such processes produce toxic by-products and huge amounts of sludge which must be disposed safely and require a large amount of oxidant chemicals. These methods are also quite expensive, energy consuming and have hard operating conditions [5-8]. Quite a few biological ways have been utilized to treat these

kinds of wastewater [2,5,8-10]. A large number of azo dyes cannot be treated by traditional aerobic ways due to their refractory character; azo dyes molecules have a large degree of complex aromatics and strong electron-withdrawing property as well. Moreover, the degradation of Azo-dye by means of photocatalysis relies upon catalyst level and is sensitive to temperature [11,12]. Electrochemical measures for azo dye removal are ecofriendly and cost-competitive alternatives to the physicochemical and biological degradation methods because of the following benefits: environmental compatibility, versatility, energy efficiency, safety, selectivity, and cost effectiveness. In addition, no consumption of chemicals and no production of sludge have been taken into account in many researches as plus factors [1,13,14].

For biodegradation of azo dye C.I. Acid Red 18, a two-step anaerobic-aerobic process is required [2,9,10]. The results of a work conducted by Mozia et al. [12] showed the amount of Acid Red 18 removal through the photocatalytic process decreased with increasing catalyst loading owing to photon flux prohibition into the reactor. Moreover, this system is sensitive to environmental conditions, particularly temperature.

There are many studies in which treatment of wastewaters containing dyes by electrochemical methods have been investigated [15-17]. Nonetheless, to our best knowledge there are quite a few researches that have dealt with Acid Red 18 removal through anodic oxidation. Song used the electrode of multi-walled carbon nanotubes to reduce acid red 18, but this study did not tackle the mineralization of the dye [18]. Another study by Parsa et al. used ex-

pensive electrodes such as platinum to remove Acid Red 18 by means of an ozone-electrolysis system in the presence of the supporting electrolyte of NaCl in a semi-batch reactor, [1]. However, in this study we tried to use a single system with continuous flow without adding any chemicals. Furthermore, in order to decrease investment cost, inexpensive electrodes were applied. Most previous studies on using electrochemical systems to treat water and wastewater and remove pollutants have been run in batch mode. A few studies have tackled continuous processes [1,4,14,19], but more researches are required. As we know, continuous processes have more application and are more practical. Of course, reaching a high and stable efficiency is difficult here. The prime objective of this work was to study the application of anodic oxidation for Acid Red 18 degradation. Thus, chemical oxygen demand (COD) removal and dye reduction as well as voltammetry experiment were followed. Current density, hydraulic retention time (HRT), Acid Red 18 initial concentration, and pH were optimized. Instantaneous current efficiency (ICE) and energy cost were also calculated.

MATERIALS AND METHODS

1. Process Mechanism

In this study, Pb/PbO_2 -as an inactive dimensionally stable anodes and high-oxygen-overvoltage anode- was employed for degradation of Acid Red 18 by anodic oxidation (see reactions 1-5) because it is an inexpensive material, commercially available and relatively easy and rapidly prepared, with low electrical resistivity, good chemical stability [20-22]. Anodic oxidation, as an advanced oxidation process (AOP) can destruct different pollutants, particularly dyes, from water and wastewater via in situ generation of very reactive species such as $HO^{•}$ [20-23]. The main mechanism in Acid Red 18 destruction is direct reaction of organic matters with physisorbed $HO^{•}$. This radical reacts weakly with the surface of Pb/PbO_2 and organic matters and removes them non-selectively. It is formed through the water molecule discharge [24].
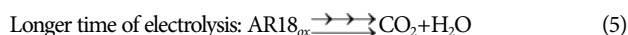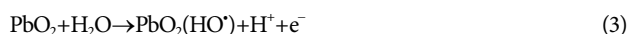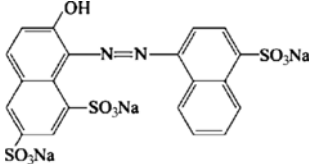
$$Pb^{2+}+2H_2O \rightarrow PbO_2+4H^++2e^- \tag{1}$$

$$PbO_2+AR18_{red} \rightarrow Pb^{2+}+AR18_{ox} \tag{2}$$

$$PbO_2+H_2O \rightarrow PbO_2(HO^{•})+H^++e^- \tag{3}$$

$$PbO_2(HO^{•})+AR18_{red} \rightarrow PbO_2+AR18_{ox} \tag{4}$$

$$\text{Longer time of electrolysis: } AR18_{ox} \xrightarrow{\quad\quad} CO_2+H_2O \tag{5}$$

Table 1. General characteristics of C.I. Acid Red 18 [2]

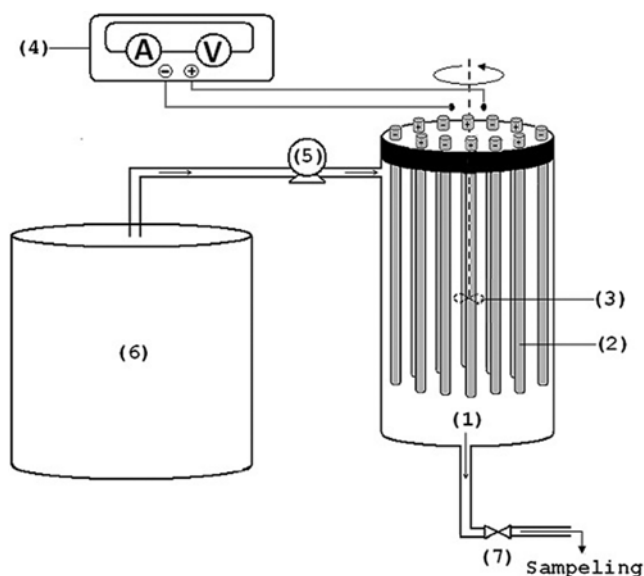| Parameter	Value
Molecular formula	$C_{20}H_{11}N_2Na_3O_{10}S_3$
Molecular weight	604.5 (g/mol)
COD of 1 g-AR18/L	597±17 (mg/L)
λ_{max}	507 (nm)
Chemical structure	

Fig. 1. Schematic diagram of the continuous electro-degradation of Acid Red 18 by anodic oxidation process.
(1) Electrochemical cell   (5) Direct current pump
(2) Pair electrodes   (6) Surge vessel
(3) Mechanical mixer   (7) Valve
(4) DC power supply

2. Reagents

Acid Red 18 (>99% purity) was purchased from Alvan Sabet Co., Hamadan, Iran. The structural formula and general characteristics of the dye are given in Table 1. All other chemicals, including NaOH, Na_2SO_4, H_2SO_4, HCl (15%wt) and NaCl, were of analytical grade and obtained from Merck Co., Germany. Acid Red 18 was used without additional treatment. Concentrations between 0.17 and 1.9 mM of the dye were prepared. Sulfuric acid and sodium hydroxide were used to adjust the pH of the solutions.

3. Experimental Unit

A schematic diagram of the continuous electro-degradation of Acid Red 18 is shown in Fig. 1. The pilot system is comprised of seven main compartments: cylindrical electrochemical cell, pair electrodes, mechanical mixer, DC power supply, direct current pumps, surge vessel and valve. The electrochemical cell (16×30 cm) was made of acrylic material with an effective liquid volume of 5 L. The flow rates of the pilot plant were in the range of 0.42-4.5 cm^3/S. Nine monopolar rods Pb/PbO_2 electrodes were placed per cathode and anode with dimensions of 2×35 cm. The distance between the electrodes (1.2 cm) and effective electrode area (0.23 m^2) were fixed in all experiments. The electrodes were installed at 5 cm from the bottom of the cell. To maintain appropriate mixing of the solution, the electrodes were placed at the sides of the cell with a 2 cm distance from the internal wall and a mechanical mixer was placed in the center of the cell. All experiments were conducted under mixing (300 rpm) to ensure good dispersion of the solution. The electrodes were also connected to the terminals of a direct current power supply (Adak, ps_405, Hamadan Kit Co., Iran) characterized by the ranges 0-100 A for current and 0-150 V for voltage.

4. Preparation of the Electrodes

The electrodes were rod-shaped and provided manually. For prep-

aration of Pb/PbO_2 electrodes and before embedding PbO_2 on the surface of the rods, some actions were done as follows: because the surface of the rods was covered with sand, first, the surface of the electrode was polished and the particles were separated by using acetone and it was entirely smoothed. Next, an alkaline solution containing sodium carbonate (20 g/L), sulfuric acid (2 g/L), sodium hydroxide (50 g/L), and trisodium orthophosphate (20 g/L) was employed to clean the surface of the electrodes completely. Furthermore, to have the electrodes without any oxides or scales and the film of PbO_2 embedded on the Pb electrode, first, the electrodes were kept in a solution consisting of nitric acid (400 g/L) and hydrofluoric acid (5 g/L) and then polished in boiled oxalic acid solution (100 g/L) for 5 min [25]. So as to prepare the Pb/PbO_2 electrode, Pb rod electrodes were put in sulfuric acid (10%) at the current density of 10 mA/cm² at 25 °C for 90 min [20]:

$$Pb+SO_4^{2-} \rightarrow PbSO_4+2e^- \quad (6)$$

$$PbSO_4+2H_2O \rightarrow PbO_2+SO_4^{2-}+4H^++2e^- \quad (7)$$
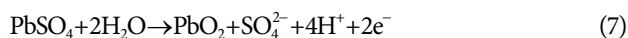
Prior every run, the electrodes were cleaned with a solution of HCl (15%wt) and then washed by distilled water.

5. Analytical Methods

The procedure employed in this study consisted of operating the system with different HRTs (t=20-200 min), current density (i=1.7-15.5 mA/cm²), initial pH values (2-11), and Acid Red 18 concentrations (C=0.17-1.9 mM), which created a COD concentration of 50-700 mg/L. Note that the main parameters were optimized through one-at-a-time method [14,26]; first, pH was optimized: the values of 2.0, 3.0, 4.0, 5.0, 6.0, 7.0, 8.0, 9.0, 10.0 and 11.0 were used. Since pH had no effect on electro-degradation, neutral pHs were used to optimize current density. After this stage, the optimum amount of current density (8.6 mA/cm²) and neutral pH were used to gain optimum HRT. Moreover, each 20 min a sample was taken and examined to investigate the amount of dye and COD removal. All experiments were done at 21±3 °C and conducted three times and the errors were between 0.72 and 0.91, being calculated with intraclass correlation coefficient. COD was carried out in accordance with the Standard Methods for Examination of Water and Wastewater (colorimetric method/photometry) [27]. The pH value was measured by means of a portable pH meter (Orion 250A pH-meter). Electrical conductivity (EC) and total dissolved solid (TDS) were measured with a Hach conductivity/TDS meter (model 44600, Hach Chemical, Stanford, CT). The color intensity of the feed and effluent samples was analyzed by a spectrophotometer (Perkin Elmer Lambda 20). To determine dye concentration, the absorbance of the test samples at the maximum absorbent wavelength of Acid Red 18 (λ_{max}: 507 nm) was measured through a UV/Vis spectrophotometer (Hach DR-4000).

Cyclic voltammetry, controlled-potential coulometry and preparative electrolysis were conducted by using an Autolab model PGSTAT 20 potentiostat/galvanostat. The working electrode applied in the voltammetry experiment was a glassy carbon disc (1.8 mm diameter) and platinum wire was applied as the counter electrode.

Removal efficiency of COD and color content was calculated using the following equation:

$$R(\%)=\frac{C_i-C_t}{C_i} \times 100 \quad (8)$$

where, C_i and C_t are initial and final concentrations of COD and dye in the wastewater, respectively.

COD data allow the electrochemical energy consumption (EEC, kWh/kg COD) to be determined for each treated solution at any given time [20]:

$$EEC=\frac{VIt}{3600 \times 10^3} \times \frac{1}{\Delta C \times V_R \times 10^{-6}} \quad (9)$$

where, V is the average cell voltage (V), I is the applied current (A), t is the electrolysis time (s), ΔC is the difference in COD (mg/L) and V_R is the solution volume (L).

On the basis of the COD values, the ICE was calculated as [28]:

$$ICE=\frac{|(COD)_t-(COD)_{t+\Delta t}|}{8I\Delta t}FV \quad (10)$$

where, $(COD)_t$ and $(COD)_{t+\Delta t}$ are the COD concentration (mg/L) at times t and t+Δt (s), respectively, F is the Faraday constant (96,485.3 C/mol) and 8 is the equivalent mass of oxygen (g mol^{-1}).

RESULTS AND DISCUSSION

1. Effect of Operating Parameters
1-1. The Influence of pH

To investigate pH impact on decolorization and COD removal, bufferic solutions were used. Fig. 2(a) shows that at the current
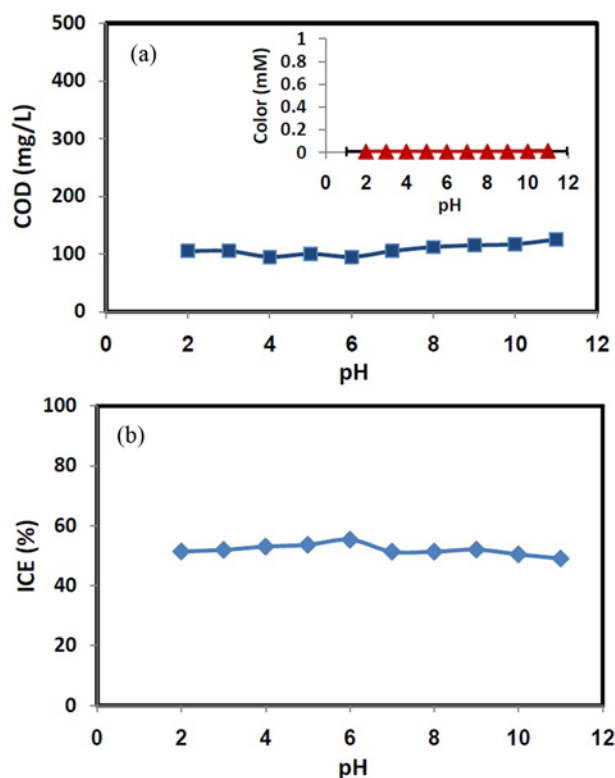

Fig. 2. Effect of initial pH on (a) COD and color removal, (b) instantaneous current efficiency: i=8.6 mA/cm², t=120 min, COD =500 mg/L and color=1 mM.

density of 8.6 mA/cm^2 and HRT of 120 min, pH variations (pH= 2-11) did not have a significant effect on both COD removal and Acid Red 18 decolorization; as a whole in all pHs, the amount of COD removal and decolorization were 76.5-81.1% and 99.9%, respectively. The variations of pH were not significant; over the process, the pH value increased slightly which it was not more than 1 unit. Moreover, ICE was from 51.3 to 55.3%. As can be seen from Fig. 2(b), pH value was not a controlling variable over the process. Similar results were obtained by Song et al. [21,22] that showed pH value did not have a significant effect on decolorization and COD removal of 4-chloro-3-methyl phenol and azo dye C.I. Reactive Red 195 through anodic oxidation. Same efficiency for dye and COD removal may be owing to the same production of oxidants during electrochemical reactions. It is an advantage of this method when the pH value of different wastewaters fluctuates; in this case, it is not needed to adjust pH. Cong et al. [29] obtained similar results that hydroxyl radical is generated under neutral, acidic and basic conditions (reactions 11 and 12).

$$H_2O \rightarrow HO^{\bullet} + H^+ + e^-$$ (11)

$$OH^- \rightarrow HO^{\bullet} + e^-$$ (12)

1-2. The Influence of Current Density

As can be seen from Fig. 3(a), up to 99.9% of the Acid Red 18 decolorization and more than 80.0% of the COD removal occurred at the current density of 8.6 mA/cm^2 (constant passed charge of 46.6 C/cm^2). An increase in current density led to an increase in
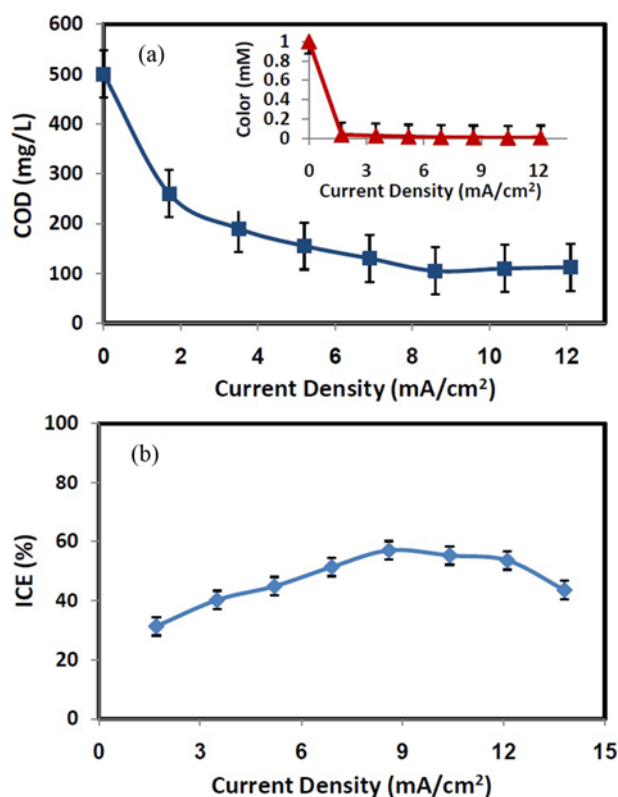

Fig. 3. Effect of current density on (a) COD and color removal and (b) instantaneous current efficiency at 46.6 C/cm^2: COD=500 mg/L and color=1 mM.

decolorization and mineralization efficiency owing to oxidants production increase, particularly HO$^{\bullet}$ generated from water oxidation. COD removal and decolorization Acid Red 18 grew until current density up to 8.6 mA/cm^2. However, the pattern was reversed after this figure. This is also confirmed by ICE data (see Fig. 3(b)). Song et al. [22] reported that current density had both positive and negative effect, and efficiency was low at high current densities for azo dye C.I. Reactive Red 195 electro-degradation. Mook et al. [30] claimed that efficiency of destruction of organic matters in synthetic wastewater decline at high current densities and as well as high detention times is due to a rise in water anodic oxidation and oxygen generation instead of HO$^{\bullet}$. As regards decolorization Acid Red 18 the electro-oxidation methods was very effective and the dye was removed well even at current density lower than 8.6 mA/cm^2 (1.7-6.9 mA/cm^2).

Mineralization current efficiency results indicated in the beginning of the reaction mineralization occurred quickly at a low current density of 5.2 mA/cm^2, whereas at high current density (10.4 mA/cm^2) the rate of mineralization current efficiency decreased. Song et al. [21] claimed that with increasing current density the mineralization efficiency rose quickly and then went down gradually, suggesting that the mass transfer of the dye to the electrode surface could not be ignored. Overall, organic matter mineralization is controlled by mass transfer or by both chemical reaction and mass transfer. Similarly, mineralization current efficiency at higher current density was lower than those at lower current density; previous studies confirm this and show that high current density leads to low mineralization current efficiency and high energy consumption [21,22]. The bottom line is that a rise in current density over optimized points does not result in an increase in efficiency.

1-3. The Influence of Hydraulic Retention Time

The investigation of HRT indicated that the more HRT the more efficiency. At the optimized current density (8.6 mA/cm^2) the highest percentages of COD removal (36.4-81.0%) and decolorization (73.5-99.9%) were obtained at HRTs of 20-180 min, respectively. Nonetheless, at HRTs over 160 min the efficiency declined and, in turn, it resulted in energy consumption increase. ICE was high at the beginning (the first 20 min of the reaction). The findings of other studies have illustrated that intermediate components are generated during electrochemical reactions, which are degraded slowly [21,30]. Fig. 4(a) illustrates that with increasing HRT, despite approximately complete dye reduction (99.9%), only 81.0% of COD was removed.

Non-active electrodes like PbO$_2$ do not participate in direct destruction of organic matter on catalytic sites, and consequently mineralization is not controlled by adsorption processes. Song et al. [21] explained the mass transfer mechanism and chemical reactions control removal processes. They presented that in the presence of KI, which is used to scavenge HO$^{\bullet}$, the amount of organic matters removal decreased dramatically because of indirect oxidation of these components by created oxidants; another study confirms this [31]. With raising HRT (more than 160-180 min), the efficiency declined because any unsuitable side-reaction, such as electrolysis of water and oxygen evolution from HO$^{\bullet}$, would compete with the electro-oxidation of the contaminant; of course, the occurrence of other adverse reactions which lead to by products
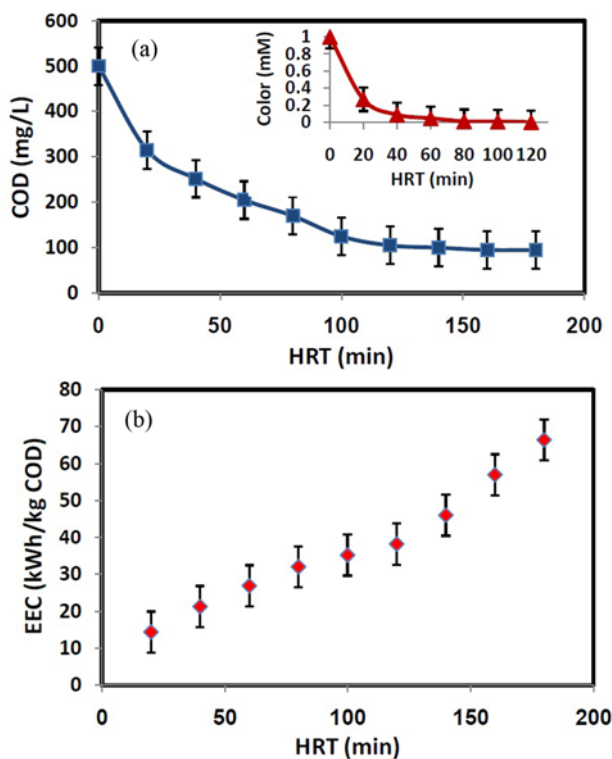
Fig. 4. Effect of hydraulic retention time on (a) COD and color removal and (b) electrochemical energy consumption: $i_{optimized}$= 8.6 mA/cm^2, COD=500 mg/L and color=1 mM.

has also been reported [32]. The efficiency dropped owing to factors as follows: parasite reactions occurrence oxidizing PbO_2 ($HO^•$) to weaker oxidants, by-product generation like (poroxydisulfates) $S_2O_8^{2-}$ in the presence of SO_4^{2-} [4,32].

In this study, PbO_2 was selected. Although PbO_2 used in our study has a lower efficiency in comparison with boron-doped diamond (BDD), it is not expensive and not fragile in spite of other electrodes like nano-crystalline PbO_2, carbon, and graphite felt and, more importantly, it has a high oxidation power and approximately entire decolorization and COD removal [30,33].

The figures of optimized amounts - HRT and current density - were used to calculate energy consumption (see Fig. 4(b)). In this work for 20-180 min the amount of energy consumption ranged between 14.4 and 66.4 kWh/kg COD; it should be noted that at the optimum conditions the majority of COD (79.5%) was removed only with 38.2 kWh/kg COD of energy consumption in 120 min.

The upside of applying the electrochemical method, of course, is that it requires little detention time (maximum 140 min) compared to the two following processes: photocatalytical and biological, which need a high detention time from a few hours to quite a few days [2,9-12]. In spite of biological measures in which operating parameters such as exact pH, temperature, COD/N/P ratio and so forth, should be controlled precisely, the electrochemical method is not sensitive to pH changes and, more importantly, it is easily controllable by current density and HRT. Another important point is that biological processes are not economical in small scales because the volume of wastewater is very slow and has high loading organic matters. However, on the other hand, the main downside

of electrochemical methods is that they cannot still be applied at high volume of wastewater because of high energy consumption demand. In the current study, the dye and COD were removed by 99.9% and 80.0%, respectively, without adding any extra chemicals to use a single system with continuous flow despite another recently published study, in which Acid Red 18 was treated by ozone-electrolysis process as a hybrid method and 1 g/L of NaCl was used as the supporting electrolyte, which showed that despite the fact that this system had a very good performance in decolorization, TOC was removed only up to 50% in the solution containing 100 mg/L Acid Red 18. Having a stable efficiency in continuous flow and optimization of operating variables, especially HRT, is much harder than batch and semi-continuous systems. However, we reached a very good efficiency and stability. Continuous flow can increase contact between electrode surfaces and dye and in turn the efficiency rises.

1-4. The Influence of Initial Concentration

By increasing initial concentration, the efficiency of COD and dye removal decreased. Previous studies confirmed this: Song et al. [22] and An et al. [34] explained that there is a downward trend by raising concentration. In this study, the rate of decolorization dropped when the concentration was raised from 0.17 to 1.9 mM: this occurred when the fixed passed charge of 46.6 C/cm^2 was used, while the efficiency went up by increasing initial concentration, passed charge was also raised over 61.9 C/cm^2. This decrease in the efficiency is attributed to $HO^•$/dye concentration decline. The results of our study showed that this system is able to work on high concentrations of the dye, through controlling the operating parameters, particularly HRT, which results in more production of $HO^•$. In this case, the approach can remove Acid Red 18 even at very high concentrations of the dye. In view of the fact that organic matter destruction on the electrode surface is done by physisorbed $HO^•$, at low concentrations the rate of diffusion is low and vice versa. Thus, when low concentrations are used, the electrochemical reaction happens more quickly than the diffusion. If the initial concentration increases, more organic matters are transferred to electrode surface, and in turn the content of COD removal goes up. In this case, the created $HO^•$s are limiting and the treatment efficiency would decrease with increased initial content of the dye.

2. Voltammetry Study

Degradation of Acid Red 18 was also studied by the voltammetric techniques. Constant current electrolysis (46.6 C/cm^2) was carried out in an aqueous solution containing 1.7 mM of Acid Red 18. The electrolysis progress was monitored using cyclic voltammetry (Fig. 5). In this figure, the curve shows one anodic peak A_1 at 0.82 V vs. Ag/AgCl(sat) in the positive-going scan and two cathodic peaks C_1 and C_2 at 0.57 and 0.23 V vs. Ag/AgCl(sat), respectively, in the negative-going scan. Anodic peak current (I_{pA1}) is obtained at 25.3 μA at the beginning of electrolysis, which may be attributed to the oxidation of -N=N- group present in dye [35]. As shown, during electrolysis, with the decrease in height of the anodic peak A_1 and its cathodic counterpart (C_1), two new anodic (A_2 and A_3), and one cathodic peak (C_3) which is counterpart of A_3, appear and the height of them increases slightly. All initial anodic and cathodic peaks (A_1, C_1 and C_2) disappear and only anodic and cathodic peaks A_2, A_3 and C_3 remain, at the t=120 min (Q=38.1 C/cm^2). Since the
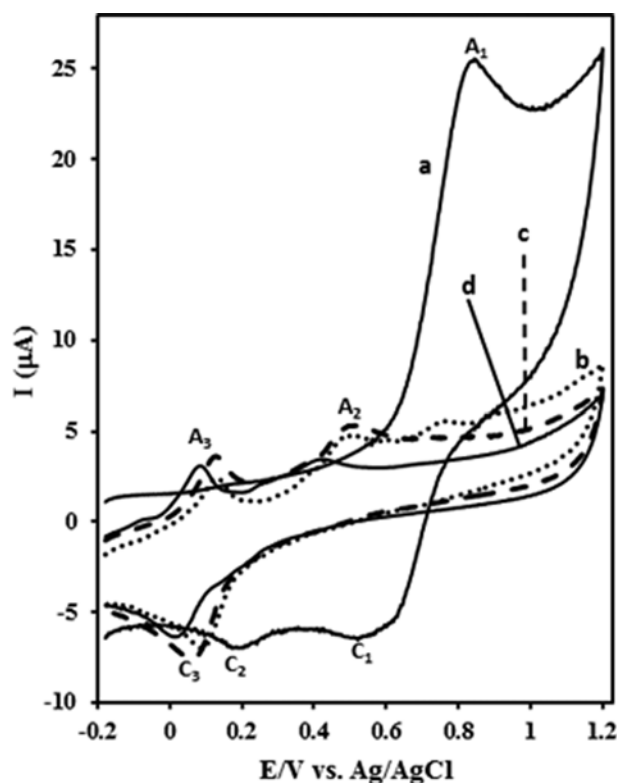
Fig. 5. Cyclic voltammograms of Acid Red 18 in solution containing C_{AR18}=1.7 mM. and bufferic pH=4 at a glassy carbon electrode (1.8 mm diameter) during constant-current electrolysis: $i_{optimized}$=8.6 mA/cm², t=0, 60, 120 and 180 min and Scan rate 100 mV s⁻¹ in 25±1 °C.

anodic peak current (I_{pA1}) is directly proportional to dye concentration, the decrease in current reveals the dye degradation.

Following our experience in electrochemical study of *ortho* and *para*-dihydroxybenzene [36-39], we can assume that the reversible redox peaks, A_3/C_3, can be assigned to the naphthalene-1,4-dione/ naphthalene-1,4-diol redox couple or other polyphenol compounds containing two hydroxyl groups in *para*-position [40]. In addition, the anodic peak A_2 at 0.48 V can be attributed to the irreversible oxidation of naphthalene-1,2-diol to naphthalene-1,2-dione or other

polyphenol intermediates with two hydroxyl groups in *ortho*-position (Fig. 6) [41]. Difference in the electrochemical behavior of the *ortho* and *para* dihydroxybenzenes relates to the stability of their associated quinones. The electrochemically generated *ortho*-quinones are very reactive in the time scale of cyclic voltammetry and participate in the following chemical reactions [42] while, *para*-quinones are more stable [43].

By continuing the electrolysis for longer periods, at the current density of 8.6 mA/cm², all new anodic and cathodic peaks A_2, A_3 and C_3 decrease in height (Fig. 5, curve d) and eventually disappear. This confirms mineralization of produced electroactive intermediates, which are generated during dye degradation.

CONCLUSION

Anodic oxidation was successfully used to treat Acid Red 18 by using Pb/PbO₂ electrodes. Complete Acid Red 18 decolorization (99.9%) and COD removal (80.0%) were obtained, which can be due to the contribution of multiple oxidation mechanisms, especially oxidation of organic matter in solution via HO•s that is generated from water oxidation. The findings showed that the operating parameters play an important role in Acid Red 18 treatment and COD removal, and measuring the optimized conditions can result in an increase in the efficiency. At the current density lower than the optimum point (8.6 mA/cm²), mineralization current efficiency was high on the condition that HRT was high, but at current density higher than the optimum point there was not a significant growth in the efficiency and it led to energy consumption increase.

Unlike conventional methods, anodic oxidation does not need other supplementary process and chemicals. The system does not lead to by-products formation and has a better efficiency at a low detention time, and also the voltammetry study confirmed that all intermediate products disappear.

ACKNOWLEDGEMENTS
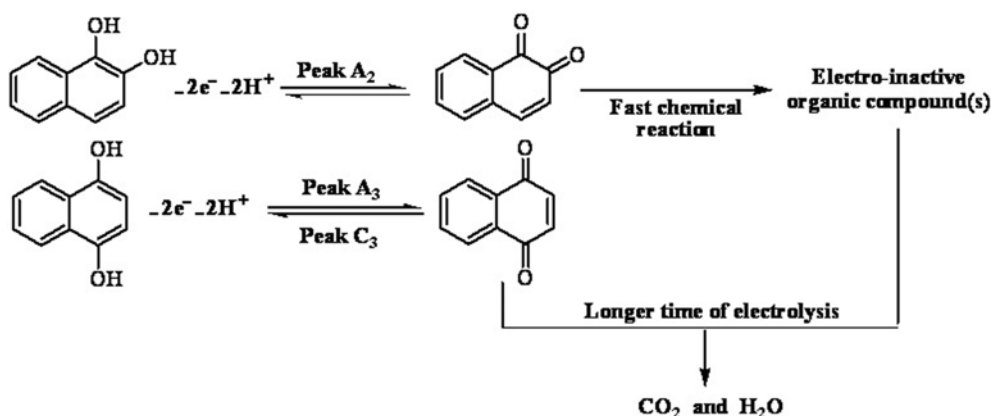
Fig. 6. Pathways to mineralization and production of intermediates during electro-oxidation of Acid Red 18.

REFERENCES

1. J. Basiri Parsa, M. Golmirzaei and M. Abbasi, *J. Ind. Eng. Chem.*, **20**, 689 (2014).
2. E. Hosseini Koupaie, M. Alavi Moghaddam and S. Hashemi, *J. Hazard. Mater.*, **195**, 147 (2011).
3. S. S. Martínez and E. V. Uribe, *Ultrason. Sonochem.*, **19**, 174 (2012).
4. E. J. Ruiz, C. Arias, E. Brillas, A. Hernández-Ramírez and J. Peralta-Hernández, *Chemosphere*, **82**, 495 (2011).
5. S. Asad, M. Amoozegar, A. A. Pourbabaee, M. Sarbolouki and S. Dastgheib, *Bioresour. Technol.*, **98**, 2082 (2007).
6. H. Lin, H. Zhang, X. Wang, L. Wang and J. Wu, *Sep. Purif. Technol.*, **122**, 533 (2014).
7. M. Shirzad-Siboni, S. J. Jafari, O. Giahi, I. Kim, S. M. Lee and J. K. Yang, *J. Ind. Eng. Chem.*, **20**, 1432 (2014).
8. A. Pandey, P. Singh and L. Iyengar, *Int. Biodeter. Biodegr.*, **59**, 73 (2007).
9. E. Hosseini Koupaie, M. Alavi Moghaddam and S. Hashemi, *Bioresour. Technol.*, **127**, 415 (2013).
10. E. Hosseini Koupaie, M. Alavi Moghaddam and S. Hashemi, *Int. Biodeter. Biodegr.*, **71**, 43 (2012).
11. S. Mozia, M. Tomaszewska and A. W. Morawski, *Desalination*, **198**, 183 (2006).
12. S. Mozia, M. Tomaszewska and A. W. Morawski, *Desalination*, **185**, 449 (2005).
13. G. Kazem, G. Azarian, D. Nematollahi, A. R. Rahmani and H. Zolghadrnasab, *Res. J. Chem. Environ.*, **16**, 98 (2012).
14. A. R. Rahmani, D. Nematollahi, K. Godini and G. Azarian, *Sep. Purif. Technol.*, **107**, 166 (2013).
15. M. Hossain, I. Mahmud, S. Parvez and H. M. Cho, *Environ. Eng. Res.*, **18**, 157 (2013).
16. W. C. Lin, C. H. Chen, H. Y. Tang, Y. C. Hsiao, J. R. Pan, C. C. Hu and C. Huang, *Appl. Catal. B-Environ.*, **140**, 32 (2013).
17. X. Florenza, A. M. S. Solano, F. Centellas, C. A. Martínez-Huitle, E. Brillas and S. Garcia-Segura, *Electrochem. Acta*, **142**, 276 (2014).
18. Y. Z. Song, *Dyes Pigm.*, **87**, 39 (2010).
19. J. Sim, H. Seo and J. Kim, *Korean J. Chem. Eng.*, **29**, 483 (2012).
20. K. Godini, G. Azarian, A. R. Rahmani and H. Zolghadrnasab, *J. Res. Health Sci.*, **13**, 188 (2013).
21. S. Song, L. Zhan, Z. He, L. Lin, J. Tu, Z. Zhang, J. Chen and L. Xu, *J. Hazard. Mater.*, **175**, 614 (2010).
22. S. Song, J. Fan, Z. He, L. Zhan, Z. Liu, J. Chen and X. Xu, *Electrochem. Acta*, **55**, 3606 (2010).
23. I. Sirés, E. Brillas, G. Cerisola and M. Panizza, *J. Electroanal. Chem.*, **613**, 151 (2008).
24. S. Curteanu, K. Godini, C. G. Piuleac, G. Azarian, A. R. Rahmani and C. Butnariu, *Ind. Eng. Chem. Res.*, **53**, 4902 (2014).
25. H. S. Awad and N. A. Galwa, *Chemosphere*, **61**, 1327 (2005).
26. A. R. Rahmani, D. Nematollahi, G. Azarian, K. Godini and Z. Berizi, *Korean J. Chem. Eng.*, **32**, 1570 (2015).
27. W. Horwitz (Ed.), Standard Methods for the Examination of Water and Wastewater, 20th Ed., APHA, Washington, D.C. (2005).
28. H. Xu, A. P. Li, Q. Qi, W. Jiang and Y. M. Sun, *Korean J. Chem. Eng.*, **29**, 1178 (2012).
29. Y. Cong, Z. Wu and Y. Li, *Korean J. Chem. Eng.*, **25**, 727 (2008).
30. W. Mook, M. Aroua, M. Chakrabarti, C. Low, P. V. Aravind and N. Brandon, *Electrochim. Acta*, **94**, 327 (2013).
31. J. Gao, H. Zhao, F. Cao, J. Zhang and C. Cao, *Electrochim. Acta*, **54**, 2595 (2009).
32. A. R. Rahmani, K. Godini, D. Nematollahi and G. Azarian, *Desalin. Water Treat.*, **56**, 2234 (2015).
33. M. Panizza and C. A. Martinez-Huitle, *Chemosphere*, **90**, 1455 (2013).
34. H. An, H. Cui, W. Zhang, J. Zhai, Y. Qian, X. Xie and Q. Li, *Chem. Eng. J.*, **209**, 86 (2012).
35. B. Krishnakumar and M. Swaminathan, *Spectrochim. Acta A*, **81**, 739 (2011).
36. D. Nematollahi and H. Shayani-Jam, *J. Org. Chem.*, **73**, 3428 (2008).
37. D. Nematollahi, A. Amani and E. Tammari, *J. Org. Chem.*, **72**, 3646 (2007).
38. D. Nematollahi, A. Afkhami, E. Tammari, T. Shariatmanesh, M. Hesari and M. Shojaeifard, *Chem. Commun.*, **2**, 162 (2007).
39. D. Nematollahi, M. S. Workentin and E. Tammari, *Chem. Commun.*, **15**, 1631 (2006).
40. L. Yue, K. Wang, J. Guo, J. Yang, X. Luo, J. Lian and L. Wang, *J. Ind. Eng. Chem.*, **20**, 725 (2014).
41. Z. He, C. Huang, Q. Wang, Z. Jiang, J. Chen and S. Song, *Int. J. Electrochem. Sci.*, **6**, 4341 (2011).
42. H. Beiginejad, D. Nematollahi, M. Bayat, F. Varmaghani and A. Nazaripour, *J. Electrochem. Soc.*, **160**, H693 (2013).
43. H. Beiginejad, D. Nematollahi, F. Varmaghani, M. Bayat and H. Salehzadeh, *J. Electrochem. Soc.*, **160**, G3001 (2013).